TOTEM-NOTE 2004-005
May 2004

Simulation of diffractive and non-diffractive processes at the LHC energy with the PYTHIA and PHOJET MC event generators.

F.Ferro, A.Sobol
INFN, Genova, Italy
J.P.Guillaud
LAPP, IN2P3-CNRS, Annecy-le-Vieux, France

CERN-TOTEM-NOTE-2004-005
31/05/2004

Abstract

The predictions of the PYTHIA6.205 and PHOJET1.12 MC events generators for diffractive processes and minimum bias events are presented for the LHC energy. The comparison with the experimental data from the ISR, the SPS and the Tevatron is made.

1. Introduction

In the proton-proton interactions it is customary to distinguish between elastic and inelastic processes. Again, it is conventional to divide inelastic processes into diffractive and non-diffractive ones. Non-diffractive events are usually called *minimum bias events* . Diffractive processes include single and double diffractive dissociation and central diffraction. at the LHC energy it is expected a pure double pomeron exchange in the central diffractive production [1]. Thus, we can write the total proton-proton cross-section as the following series

$$\sigma_{tot} = \sigma_{elas} + \sigma_{inelas} = \sigma_{elas} + \sigma_{mb} + \sigma_{dif} = \sigma_{elas} + \sigma_{mb} + \sigma_{sd} + \sigma_{dd} + \sigma_{cd} \qquad (1)$$

Among the detectors being constructed at the interaction points of the LHC, TOTEM [2] has been designed to measure the total proton-proton cross-section, the elastic scattering and the total inelastic rate. The estimation of the background for the detectors of TOTEM and the optimization of the trigger conditions need a realistic prediction of the processes from (1).

At present, different phenomenological models are used to describe the non-diffractive and diffractive processes and some of them are implemented in the Monte Carlo simulation packages (generators), like PYTHIA, PHOJET, HERWIG, ISAJET [3, 4, 5, 6]. The comparison of the different generators for minimum bias events at the LHC energy have been made in many studies (see, for example, [7]-[9]).

This report presents a study of minimum bias and diffractive events for the LHC energy in the pseudorapidity region covered by the tracker detectors of TOTEM ($3.1 < |\eta| < 4.7$ and $5.3 < |\eta| < 6.7$). Our study compares the predictions provided by the two Monte Carlo simulation packages: PYTHIA6.205 [5] and PHOJET1.12 [6].

2. MC event generators

The PYTHIA model is described at length in [5]. Below, we point out the basic principles of the model related to the simulation of the low-p_t processes. Low-p_t processes play a dominant role in the inelastic scattering. PYTHIA uses a perturbative QCD for both low-p_t and high-p_t regions. The dominant $2 \to 2$ QCD cross sections are divergent for $p_t \to 0$ and drop rapidly at large p_t. Probably the lowest order perturbative cross section will be regularized at small p_t by colour coherence effects. In PYTHIA this low-p_t divergent is solved by two ways. In the first one, the so-called "simple" scenario, it is used a cut-off parameter p_{tmin}, i.e. $d\sigma/dp_t = 0$ for $p_t < p_{tmin}$. In the second, the "complex" scenario, all divergent terms are corrected by a factor $p_t^4/(p_t^2 + p_{t0}^2)$ and p_t^2 in α_S is replaced by $(p_t^2 + p_{t0}^2)$. This removes the perturbative QCD divergencies at low-p_t. The first is equivalent to the existence of a maximum impact parameter, b_{max}, above which there are no interactions. The second assumes that there is some matter distribution in a hadron interactions at various impact parameters. Different sets of parton distribution functions (p.d.f.) may be choosen for the proton interactions. The current version of PYTHIA (6.205) uses the default p.d.f., CTEQ5L [5].

PHOJET [6] is based on the Dual Parton Model (DPM) (see review in [14]) using another mechanisms in the low-p_t region than perturbative QCD. PHOJET can be considered as a two-component model with a smooth transition between the soft and the hard regions at some p_{tmin}. PHOJET can simulate 8 basic scattering processes separately or simultaneously. They include all processes mentioned in equation (1) as well as quasi-elastic scattering and hard direct interactions. Unlike PYTHIA, the central diffraction with double pomeron exchange is included in the PHOJET tools. PHOJET, has been tuned to the minimum bias data from CDF at 1800 GeV.

HERWIG [3] is based on the UA5 results and ISAJET [4] on the Abramovskii-Kanchelli-Gribov model. These simulation packages represent more simple models than PYTHIA and PHOJET whithout smooth connections of the soft and hard physics. In [7] it is shown that HERWIG and ISAJET have large divergence with the CDF data for its inclusive p_t spectrum as well as for its pseudorapidity distributions of charged particles.

In the following, we will only discuss PYTHIA6.205 and PHOJET1.12 generators.

3. Cross-sections

In PYTHIA, the total cross-section is calculated through the Regge theory according to the following sums of powers [15]:

$$\sigma_{tot}^{pp} = 21.70 s^{0.0808} + 56.08 s^{-0.4525}$$

$$\sigma_{tot}^{p\bar{p}} = 21.70 s^{0.0808} + 98.39 s^{-0.4525}.$$

The first term in these expressions corresponds to the Pomeron exchange and the second one to the Reggeons (ρ, ω, f, a) exchanges. Because the Pomeron has the quantum numbers of the vacuum, its couplings to the proton and anti-proton are equal, so the coefficient 21.70 is the same for σ_{tot}^{pp} and $\sigma_{tot}^{p\bar{p}}$. At high energy the Reggeon term becomes negligible, $\sigma_{tot}^{p\bar{p}} \simeq \sigma_{tot}^{pp}$, so we can use for the generator comparison the experimental data from pp as well as $p\bar{p}$. In PHOJET, the cross-section is calculated according to the two component Dual Parton Model[1] using the optical theorem [19]. PYTHIA 6.205 and PHOJET 1.12 predictions for pp total cross section are shown in fig.1. Their simulated cross sections are compared with the existing pp and $p\bar{p}$ experimental data [20]. Both generators have a good agreement in the region below 700-800 GeV. Fig.4 shows that for higher energies the predictions are different, coming up to 18 % divergence at ∼10 TeV. For the LHC energy ($\sqrt{s}$ = 14 TeV) PYTHIA 6.205 and PHOJET 1.12 predict σ_{tot}^{pp} = 101.5 mb and 119 mb, respectively (see table 1). Fig. 1 shows that PHOJET 1.12 is in agreement with the CDF data and in disagreement with the E710 and E811 data at the Tevatron energy.

The elastic cross sections calculated by both generators are shown in fig. 2 and compared with the experimental data [20]. At previously, the predictions start to diverge at

[1]The Dual Parton Model is a phenomenological realization of the large N_c, N_f expansion of QCD [16] in connection with general ideas of duality [17] and Gribov's reggeon field theory [18].

energies higher than 700 GeV (the divergence is ∼55 % at the LHC energy). PYTHIA 6.205 and PHOJET 1.12 predictions for the elastic cross section at the LHC energy are respectively 22.2 mb and 34.4 mb (see table 1). The difference between the total and the elastic cross sections giving the inelastic cross section is shown in fig. 3 for both generators and compared with experimental data. For the inelastic cross section, the divergence between the two predictions is not large (6.6 % at the LHC energy).

In fig. 5 PYTHIA 6.205 and PHOJET 1.12 calculations are compared with the avaliable experimental data for single (a) and double (b) diffractions. In PYTHIA, single and double diffractive cross sections are calculated using the triple-pomeron approximation [21, 22] in the so-called Born graph approach. But the experimentally observable diffractive cross sections are considerably smaller than the Born the graph calculations.

Although data on single diffractive cross sections have large uncertainties, the rise of the cross section from the ISR energies to the energies of the S$p\bar{p}$S and the Tevatron, see fig. 5a, cannot be explained at the Born level. In the PHOJET model, a special eikonal unitarization procedure is used to suppress the strong rise of the triple pomeron exchange. This is the reason of the large divergence between the PYTHIA and PHOJET predictions for the single and double diffractive cross sections. This divergence becomes larger at higher energies and reaches 22 % for single diffraction and 58.5 % for double diffraction at the LHC energy (see table 1).

Process	PYTHIA 6.205 σ^{pp}, mb	PHOJET 1.12 σ^{pp}, mb	Difference, %
Elastic	22.2	34.4	54.9
Inelastic	79.3	84.5	6.6
Minimum bias	55.2	68.0	23.1
Single diffraction	14.3	11.0	22.0
Double diffraction	9.8	4.06	58.5
Central diffraction	—	1.42	—
Total cross section	101.5	119	17.2

Table 1: Differences between the PYTHIA 6.205 and PHOJET 1.12 pp cross sections at $\sqrt{s} = 14$ TeV.

Central diffractive events are simulated in PHOJET only. In this diffraction process, the double pomeron exchange dominates at high energy. The PHOJET 1.12 prediction for the central diffractive cross section is shown on fig. 5c. In both generators, the minimum bias cross section is calculated according to formula (1) by subtracting the diffractive cross section from the inelastic one: the result is shown on fig. 5d. The minimum bias cross sections obtained at the LHC energy are 55.2 mb with PYTHIA 6.205 and 68 mb with PHOJET 1.12. Figure 4 summarizes the difference between PYTHIA 6.205 and PHOJET 1.12 cross sections at the LHC energy for all processes listed in (1).

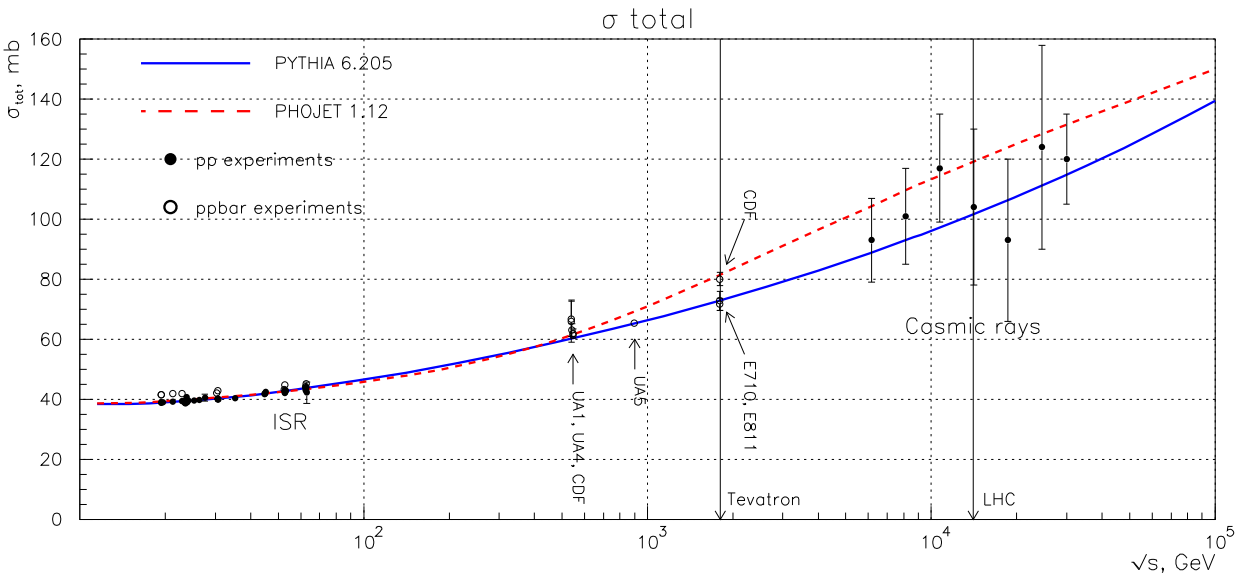

Figure 1: Predictions for the pp total cross sections from PYTHIA 6.205 (solid line) and PHOJET 1.12 (dotted line). The experimental data for total cross sections are shown for pp collisions (black circles) and for $p\bar{p}$ collisions (white circles) (data files courtesy of the COMPAS Group, IHEP, Protvino, Russia).

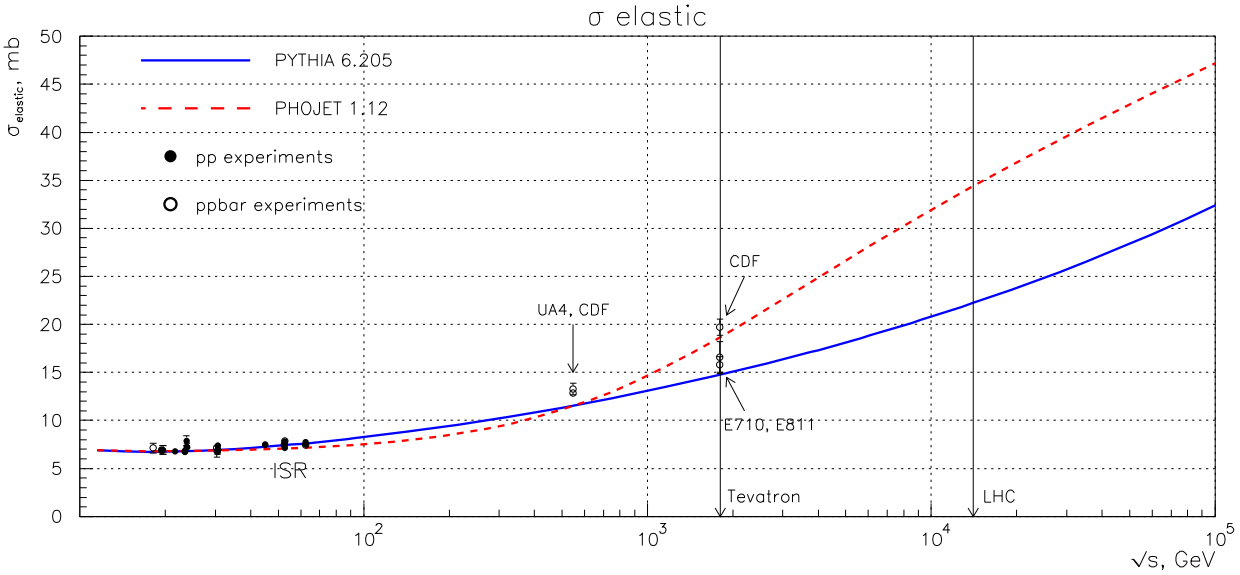

Figure 2: The same plot as in fig.1 for the elastic cross sections.

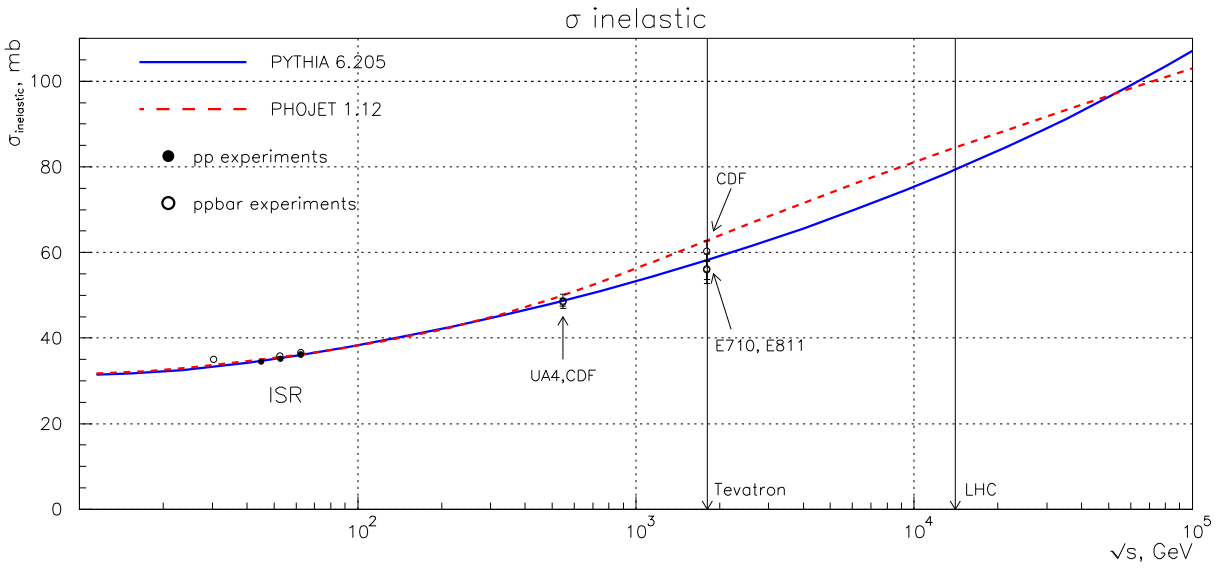

Figure 3: The same plot as in fig.1 for the inelastic cross sections.

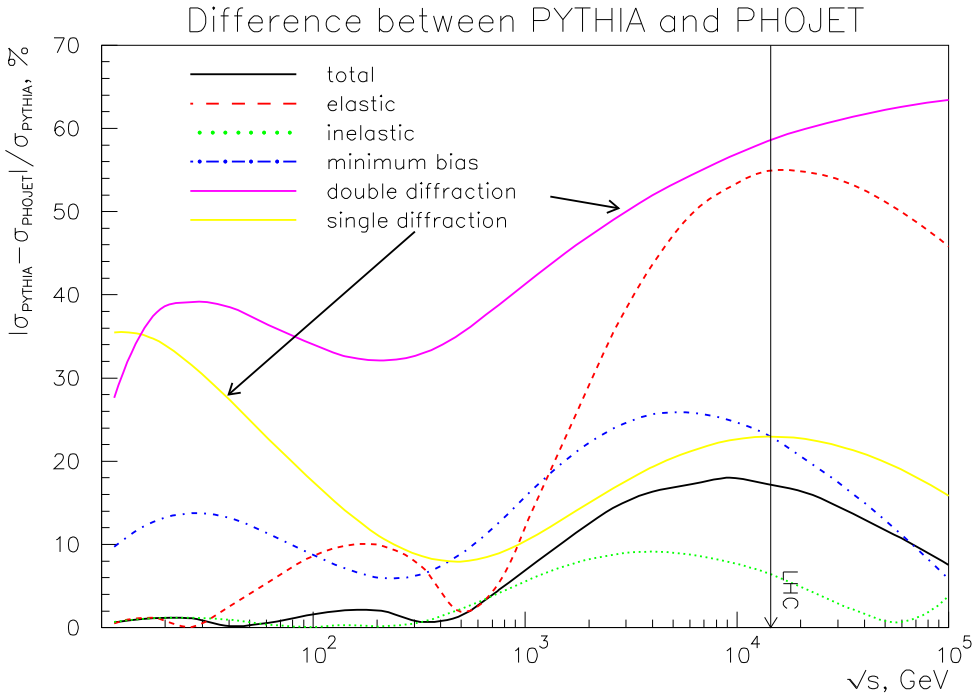

Figure 4: Difference between PYTHIA 6.205 and PHOJET 1.12.

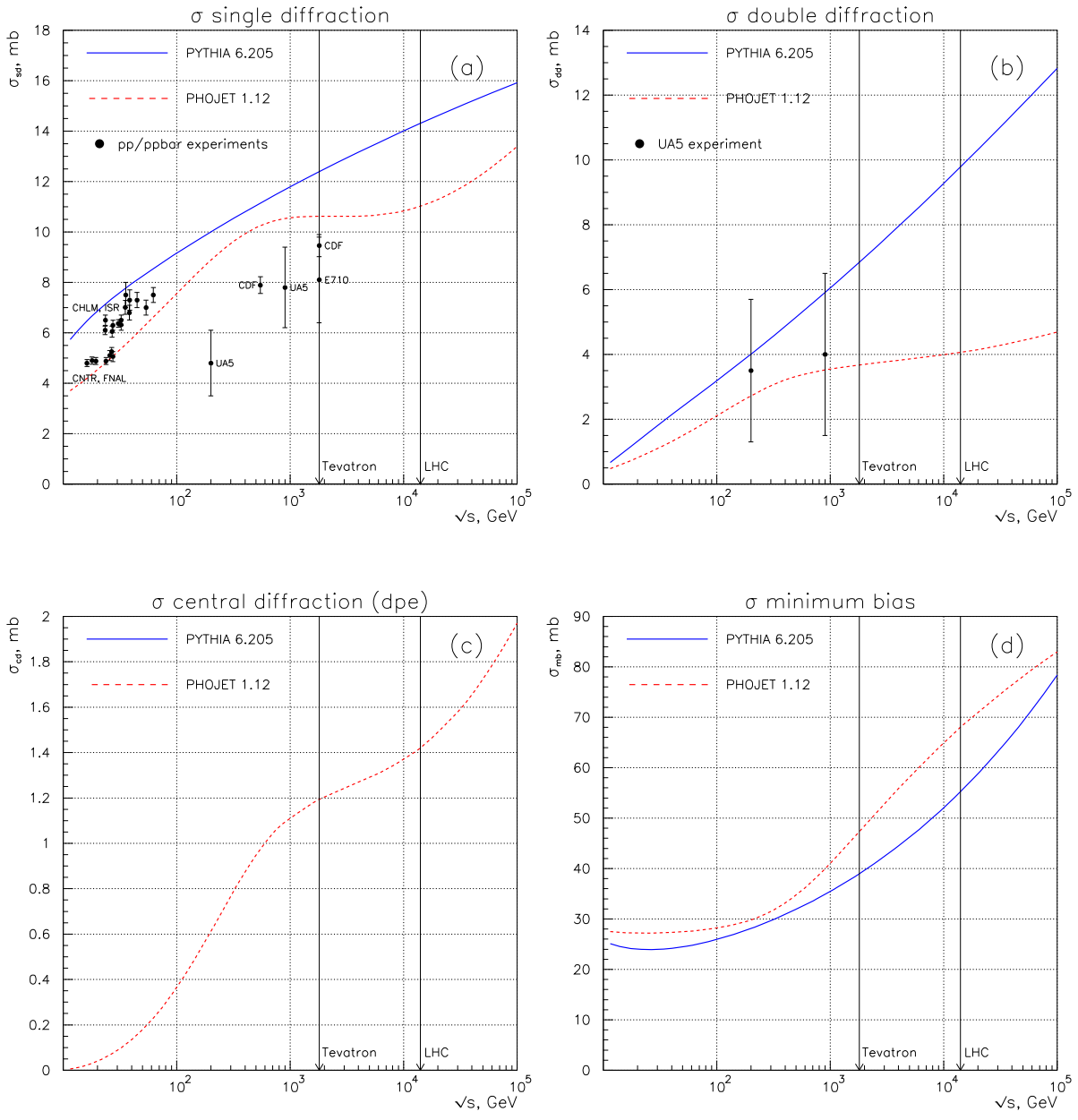

Figure 5: PYTHIA 6.205 (solid line) and PHOJET 1.12 (dotted line) cross sections for a) single diffraction, b) double diffraction, c) central diffraction and d) non-diffractive production (minimum bias). The experimental data for single diffractive cross sections [23]-[28] and double diffractive cross sections [27] are shown on figures a) and b) respectively.

4. Minimum bias

The generation of non-diffractive processes in PYTHIA can be done in different ways, varying the solution of the divergency problem (see chapter 2), the value of the cut-off parameter, the type of the parton distribution function and so on. The different scenarios of interaction can be chosen with the the keys MSTP and PARP. We studied the most commonly used scenarios (see table 2) for the non-diffractive simulations and compared them to the available data from UA5 [10] and CDF [11].

Scenario	Parameters	Explanation	p.d.f.
1, PYTHIA	MSTP(82)=1	"simple" scenario with p_{tmin} cut-off	CTEQ5L
2, PYTHIA	MSTP(82)=4	"complex" scenario (model for multi-parton interactions: varying impact parameter and a hadronic matter overlap consistent with a double gaussian matter distribution given by PARP(83) and PARP(84) (resp. default = 0.5 and 0.2) and with a continuouse turn-off of the cross section at p_{t0}=PARP(82) (see scenarios 3,4))	CTEQ5L
3, PYTHIA	MSTP(82)=4 MSTP(2)=2 MSTP(33)=3 PARP(82)=1.9	"complex" scenario 2nd order running to α_S K factor (a K-factor is introduced by a shift in the $\alpha_S(Q^2)$ argument, $\alpha_S = \alpha_S(\text{PARP}(33)Q^2)$ in accordance with [12]) p_{t0} calculation (regularization scale of the transverse momentum spectrum for multiple interactions tail) (default)	CTEQ5L
4, PYTHIA	MSTP(82)=4 MSTP(2)=2 MSTP(33)=3 PARP(82)=2.3	"complex" scenario 2nd order running to α_S K factor (see scenario 3) p_{t0} calculation (recommended by [13])	CTEQ5L
PHOJET	IPRON(1)=1	minimum bias	GRV94L

Table 2: Parameters for the different scenarios of low-p_t events generation.

The result of this comparison is shown in fig. 6. The charged particles density $dN_{ch}/d\eta$ has been calculated as a function of the pseudorapidity η for the scenarios listed in table 2 for non-single diffractive events (NSD) at $\sqrt{s}$ =200 and 900 GeV compared to the UA5 data and at $\sqrt{s}$ = 1800 GeV compared to the CDF data. Moreover, the same distributions have been calculated for inelastic events (NSD+SD) at $\sqrt{s}$ =200 and 900 GeV and compared to the UA5 data[2].

[2]There is no data for inelastic processes from CDF.

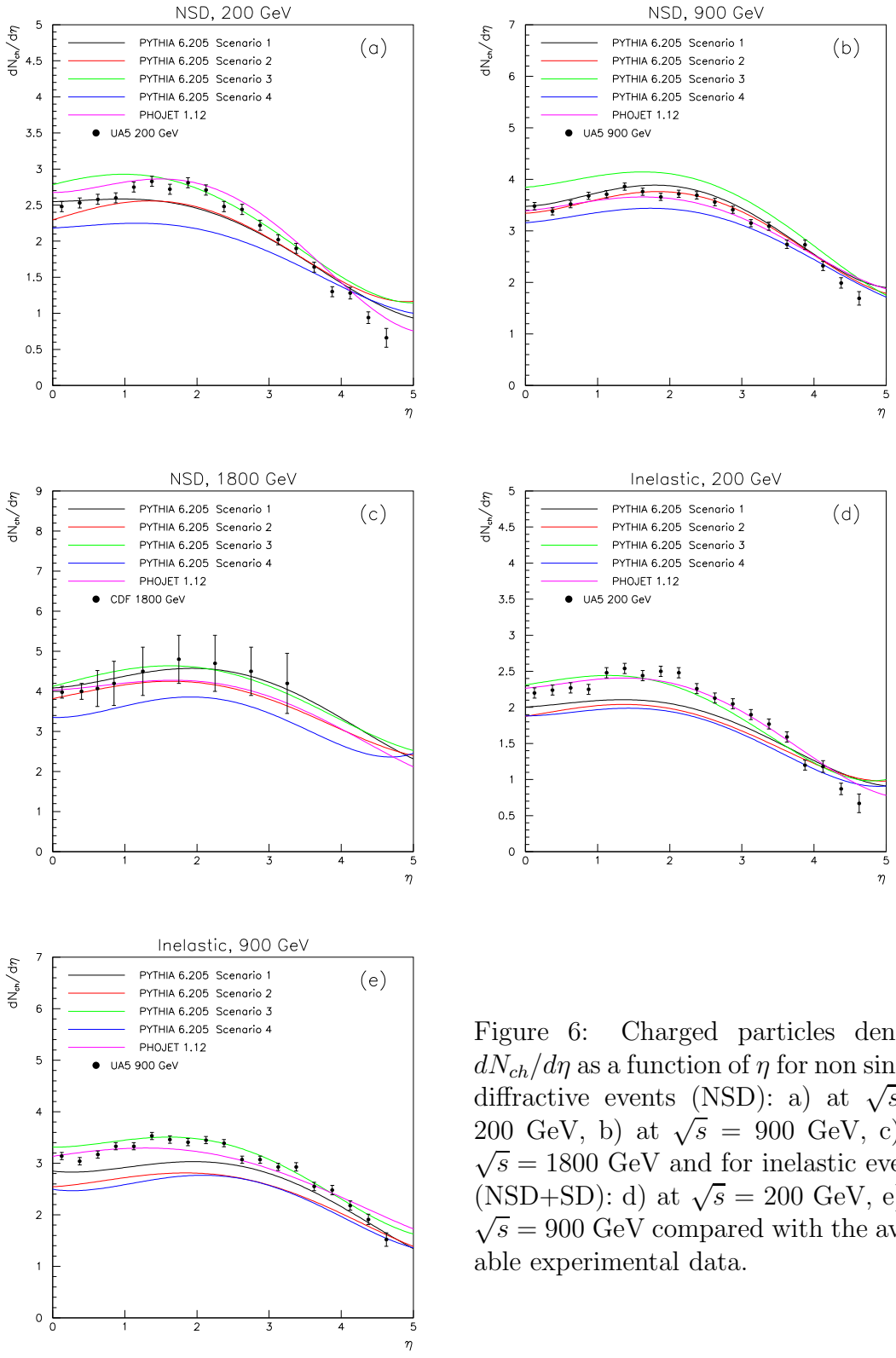

Figure 6: Charged particles density $dN_{ch}/d\eta$ as a function of η for non single-diffractive events (NSD): a) at $\sqrt{s}$ = 200 GeV, b) at $\sqrt{s}$ = 900 GeV, c) at $\sqrt{s}$ = 1800 GeV and for inelastic events (NSD+SD): d) at $\sqrt{s}$ = 200 GeV, e) at $\sqrt{s}$ = 900 GeV compared with the available experimental data.

With the scenario 3 PYTHIA 6.205 gives the best discription of the experimental data for the inelastic events at 200 and 900 GeV and for NSD events at 200 and 1800 GeV. For this reason we will use this scenario for further calculations. PHOJET 1.12, with its default parameters, perfectly describes the inelastic as well as the NSD data at all studied energies. Thus, PYTHIA 6.205 (scenario 3) and PHOJET 1.12 (default set of parameters) are in a reasonable agreement with the experimental data and among themselves.

However, there is a difference between these two MC generators at higher energy and it becomes more and more evident with the rise of the energy. The left part of fig.7 shows the central rapidity charged particles density $dN_{ch}/d\eta(\eta = 0)$ plotted as a function of c.m. energy. The PYTHIA and PHOJET predictions are compared to the NSD data from UA5 and CDF. The dotted line shows the fit to the experimental data [11]:

$$\frac{dN_{ch}}{d\eta} \mid_{\eta=0} = 0.023ln^2(s) - 0.25ln(s) + 2.5.$$

At the LHC energy this fit to the experimental data gives $\frac{dN_{ch}}{d\eta} \mid_{\eta=0} = 6.2$, when PYTHIA and PHOJET predict respectively 7.1 and 4.8 charged particles at $\eta = 0$ for the NSD events. Thus allowing to consider PYTHIA and PHOJET as high and low extreme limits for the charged particles multiplicity at energies higher than 1 TeV.

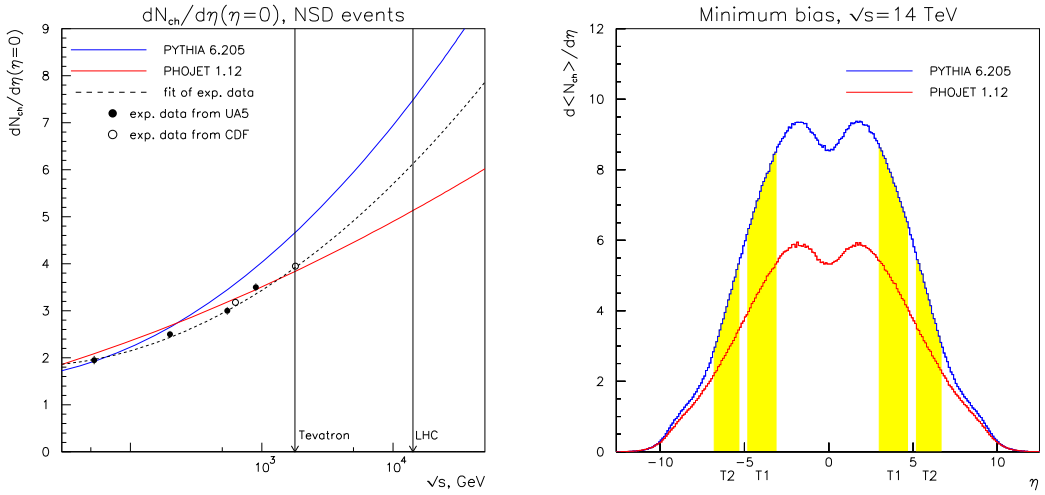

Figure 7: On the left: central rapidity charged particles density $\frac{dN_{ch}}{d\eta} \mid_{\eta=0}$ plotted as a function of c.m. energy. PYTHIA and PHOJET predictions are compared to the NSD data from the UA5 and CDF experiments. On the right: PYTHIA and PHOJET predictions for the density $dN_{ch}/d\eta$ of charged particles produced in non-diffractive processes at the LHC energy. The acceptancies of the detectors T1 and T2 of TOTEM are shown.

The right part of the fig. 7 shows the estimations of PYTHIA and PHOJET for the density of charged particles $dN_{ch}/d\eta$ produced in non-diffractive processes at the LHC energy. The charged particles densities, predicted by PYTHIA in the T1 and T2 pseudorapidity regions, are respectively 7.2 and 4.2, PHOJET gives 4.5 and 3. Table 3 shows the predictions of PYTHIA and PHOJET for the average particle multiplicity for a proton-proton minimum bias event at the LHC energy for 3 different pseudorapidity areas. PYTHIA predicts respectively 12 and 6 charged particles per event in T1 and T2, when PHOJET respectively predicts 7.6 and 3.4.

Minimum bias, $\sqrt{s} = 14$ TeV						
	T1: $3.1 < \eta < 4.7$		T2: $5.3 < \eta < 6.7$		All η	
Particles	PYTHIA	PHOJET	PYTHIA	PHOJET	PYTHIA	PHOJET
p	0.40	0.24	0.25	0.15	4.56	3.15
$\bar{p}$	0.45	0.24	0.22	0.14	3.38	1.97
n	0.80	0.47	0.49	0.28	7.24	4.66
$\pi^+\pi^-$	9.68	6.12	4.81	3.20	88.5	57.3
γ	10.9	0.59	5.41	0.25	103.6	4.9
K^+K^-	1.20	0.83	0.61	0.45	10.08	7.13
K_L	0.55	0.44	0.32	0.21	4.89	3.54
$\mu^+\mu^-$	0.003	0.003	0.00	0.00	0.023	0.018
e^+e^-	0.13	0.006	0.05	0.006	1.19	0.075
$Neutrinos$	0.004	0.003	0.001	0.001	0.018	0.017
$N_{charged}$	11.86	7.56	5.93	3.40	107.8	70.61
N_{total}	24.1	13.1	12.4	6.87	223.6	121.5

Table 3: Average particle multiplicity for a proton-proton minimum bias event obtained by PYTHIA6.205 and PHOJET1.12 at the LHC energy for different pseudorapidity areas.

5. Diffractive processes

5.1 Single diffraction

In order to compare the PHYTIA and PHOJET predictions for single diffractive production we used the $p\bar{p}$ experimental data of the UA4 Collaboration [29]. UA4 measured the pseudorapidity distributions of charged hadron production for different masses of the diffractive system. We have compared these data with PYTHIA and PHOJET (see fig. 8). We have also compared the mean charged particle multiplicity in the diffractive hadronic system measured for several masses by UA4 to the predictions of PYTHIA and PHOJET (see fig. 9). It is evident from fig. 8 and 9 that PHOJET, taking in account the contributions from the hard diffractions (minijets) and the multiple soft interactions, has

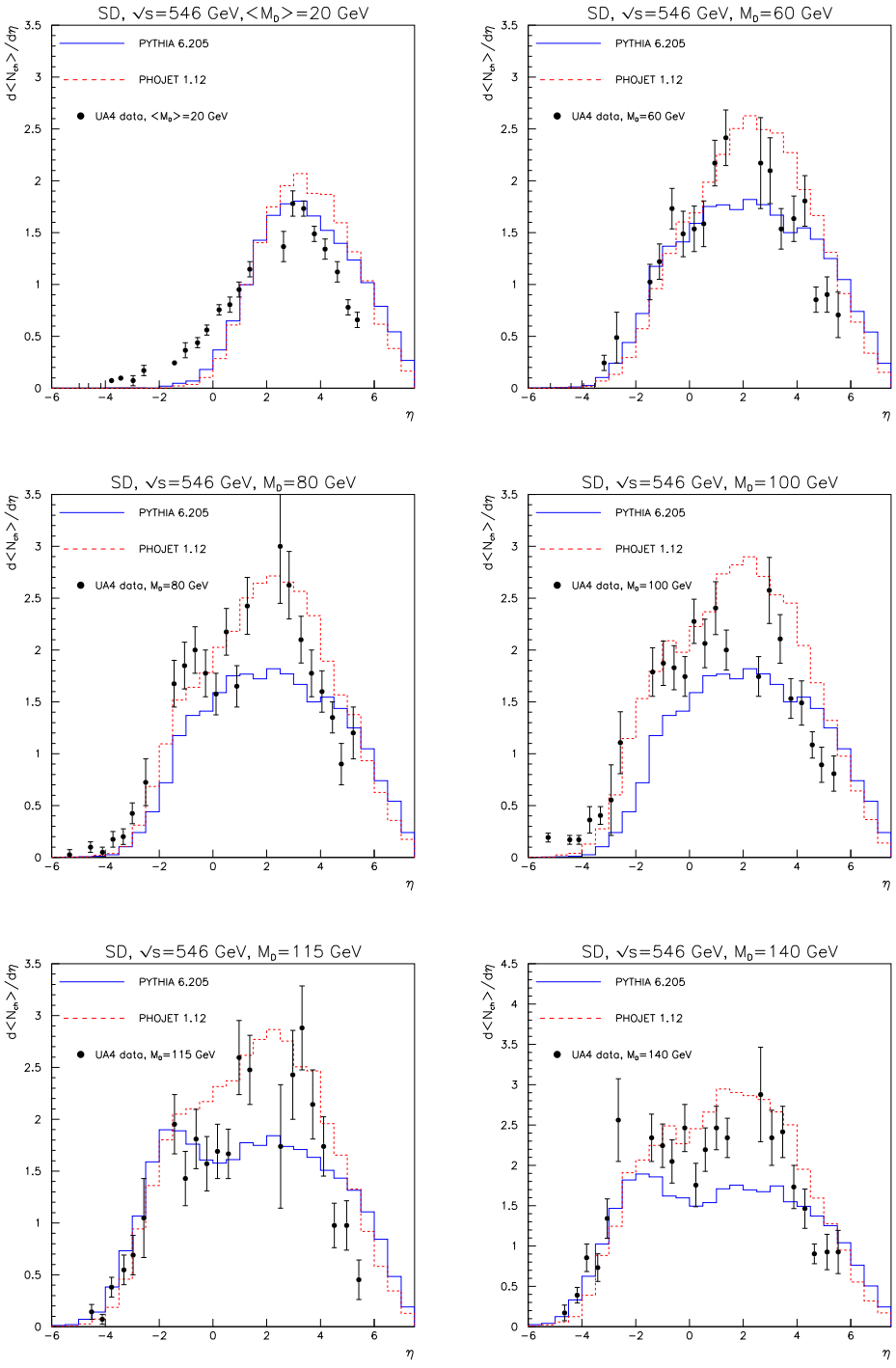

Figure 8: Pseudorapidity distributions of the charged hadrons in SD compared to the UA4 data for different masses of the diffractive system.

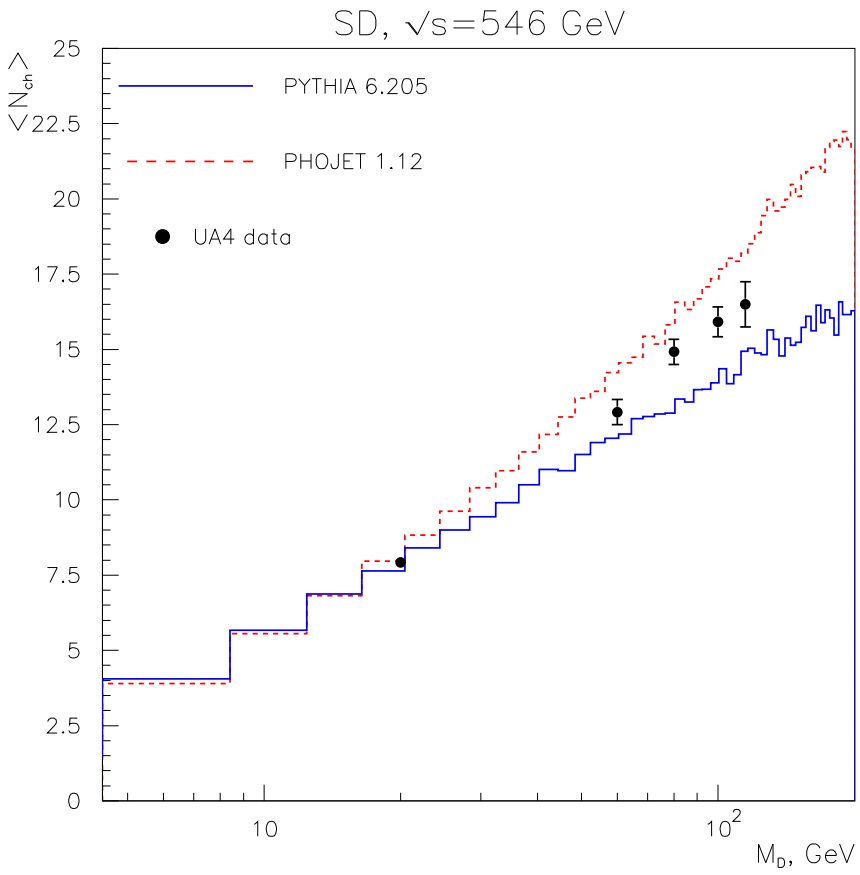

Figure 9: Average charged particle multiplicity produced in SD as a function of the invariant mass of the diffractive system compared to the UA4 data.

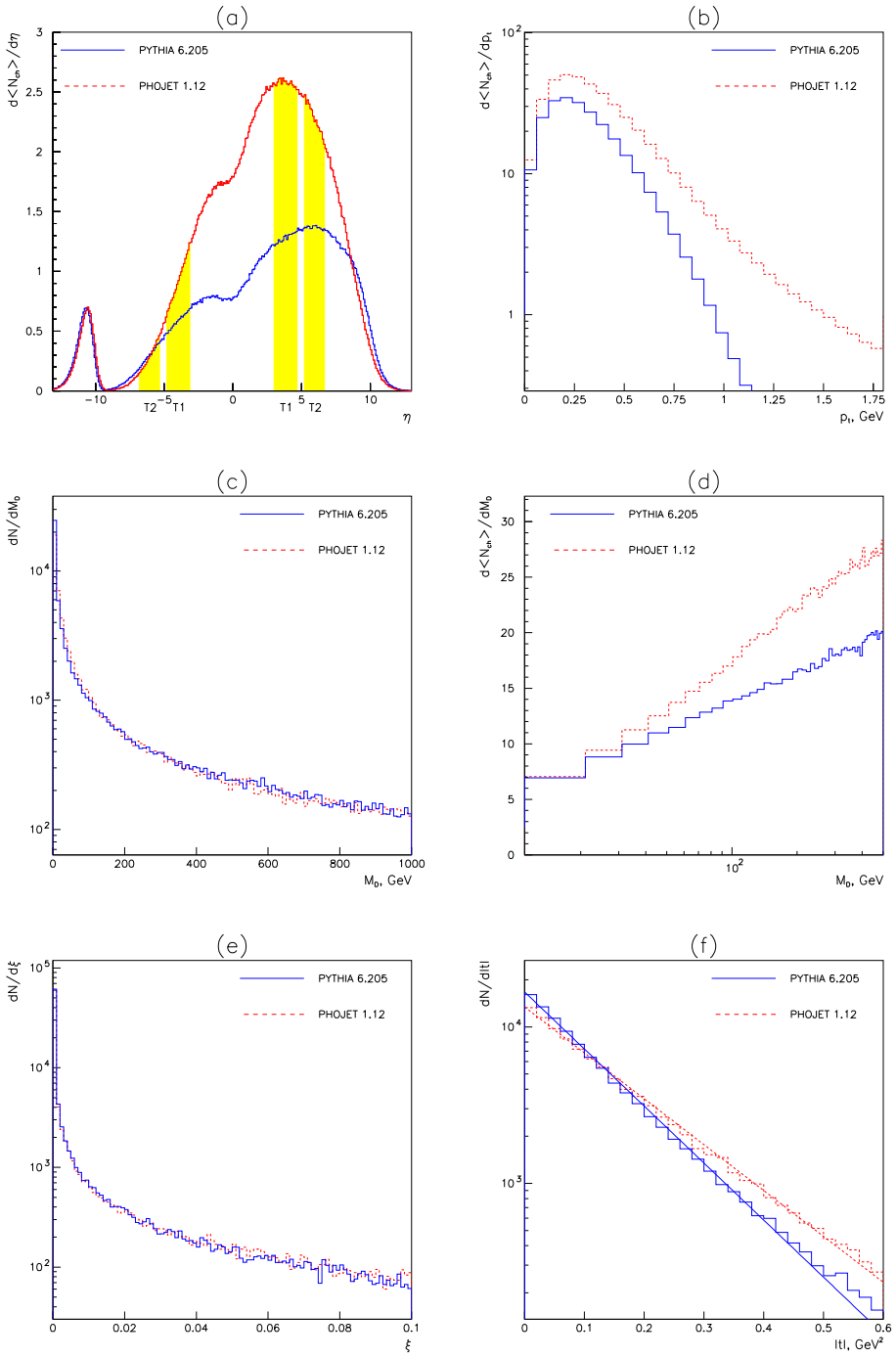

Figure 10: PYTHIA and PHOJET predictions for SD at the LHC energy: (a) charged particles pseudorapidity distribution; (b) charged particles p_t distribution; (c) mass of the diffractive system; (d) average charged particle multiplicity as a function of the diffractive system mass; (e) ξ and (f) t distributions of the scattered proton.

a better description of the data, comparing with PYTHIA, taking in account the Born term contributions only.

We have calculated with PHYTIA and PHOJET some typical distributions characterizing the single diffractive production: pseudorapidity and p_t distributions of the charged particles in the diffractive system, distribution of the diffractive mass, dependence of the average charged particle number in the diffractive system on the mass of the diffractive system, ξ and t distribution of the scattered proton, see fig. 10.

In PHYTIA as well as in PHOJET the differential cross sections, $d^2\sigma/dtdM^2$, are exponential in t and $\sim 1/M^2$:

$$\frac{d^2\sigma}{dtdM^2} \sim \frac{1}{M^2} e^{-bt}, \tag{2}$$

where M is the mass of the diffractive system, t is the transverse momentum squared of the scattered proton. t, $\xi = \delta p/p$, the relative momentum loss and ϕ, the azimuthal angle, define the kinematics of the scattered proton. In a single diffractive scattering $pp \to pX$:

$$M^2 = s\xi. \tag{3}$$

PYTHIA and PHOJET have a small difference in the t distribution (fig. 10f). The slope parameter b is equal to 8.39 in PYTHIA and to 6.75 in PHOJET.

As above mentioned, there are large divergencies between PYTHIA and PHOJET in the predictions of the charged particle multiplicity in the diffractive system, this is shown in fig. 10 (a), (b) and (d). Table 4 and fig. 10 (a) show that PHOJET predicts a multiplicity ~ 2 times larger than PYTHIA in the forward T1 and T2 pseudorapidity areas[3].

Single Diffraction, $\sqrt{s} = 14$ TeV				
	$< N_{total} >$/event		$< N_{charged} >$/event	
η region	PYTHIA	PHOJET	PYTHIA	PHOJET
T1F: $3.1 < \eta < 4.7$	4.4	7.3	2.1	4.2
T1B: $-4.7 < \eta < 3.1$	2.0	3.0	1.0	1.7
T2F: $5.3 < \eta < 6.7$	4.1	5.4	2.0	3.2
T2B: $-6.7 < \eta < -5.3$	0.8	0.7	0.4	0.4
All η	34.4	48.1	17.1	28.5

Table 4: Average particle multiplicity in the diffractive system produced in SD obtained by PYTHIA6.205 and PHOJET1.12 at the LHC energy for different pseudorapidity areas.

[3]The η distribution of the charged particles in the diffractive system produced in SD has an asymmetrical shape. We call "forward" a semisphere in the direction of the diffractive system momentum.

5.2 Double diffraction

Some distributions characterizing a double diffractive production have been obtained by PHYTIA and PHOJET (see fig. 11). These are pseudorapidity and p_t distributions of charged particles in the diffractive system, distribution of the diffractive mass, dependence of the mean charged particles number in the diffractive system on the mass of the diffractive system.

As in the case of single diffraction a large divergence in the charged particles multiplicity between PHYTIA and PHOJET is observed (see table 5), the predictions of charged particles multiplicity in the T1 and T2 pseudorapidity areas differ by a factor 2.

Double Diffraction, $\sqrt{s} = 14$ TeV				
	$< N_{total} >$/event		$< N_{charged} >$/event	
η region	PYTHIA	PHOJET	PYTHIA	PHOJET
T1: $3.1 < \eta < 4.7$	3.4	6.1	1.6	3.5
T2: $5.3 < \eta < 6.7$	3.2	4.9	1.5	2.9
All η	42.9	61.6	20.7	36.0

Table 5: Average particle multiplicity in the diffractive system produced in DD obtained by PYTHIA6.205 and PHOJET1.12 at the LHC energy for different pseudorapidity areas.

5.3 Central diffraction

Finally, we present some characteristic distributions for central diffractive production at the LHC energy (see fig. 12). They have been generated by PHOJET 1.12 with its default parameters. PYTHIA has no possibility to simulate central diffractive production.

The differential cross section is described by equation (2), but the kinematic relation (3) should be changed to

$$M^2 = s\xi_1\xi_2, \tag{4}$$

where ξ_1 and ξ_2 correspond to the 2 scattered protons in the central diffraction $pp \to pXp$. The distributions of the central diffractive mass, ξ and t of the scattered protons are respectively shown in fig. 12 (c), (e) and (f). The slope parameter b of the t-dependence is 5.73.

The density of the charged particles as a function of the pseudorapidity is shown in fig. 12a in which the left and right peaks in the region $|\eta| > 9$ are due to the scattered protons. Charged particles from the central diffractive system are distributed in the region $|\eta| < 9$. T1 and T2 acceptances are shown shaded. From table 6 one can estimate that $\sim$30 % of the charged particles from the central diffractive system fall into the T1 and T2 acceptances. Around 60% of the charged particles lie in the acceptance of the CMS tracker covering the η region from -3 to 3.

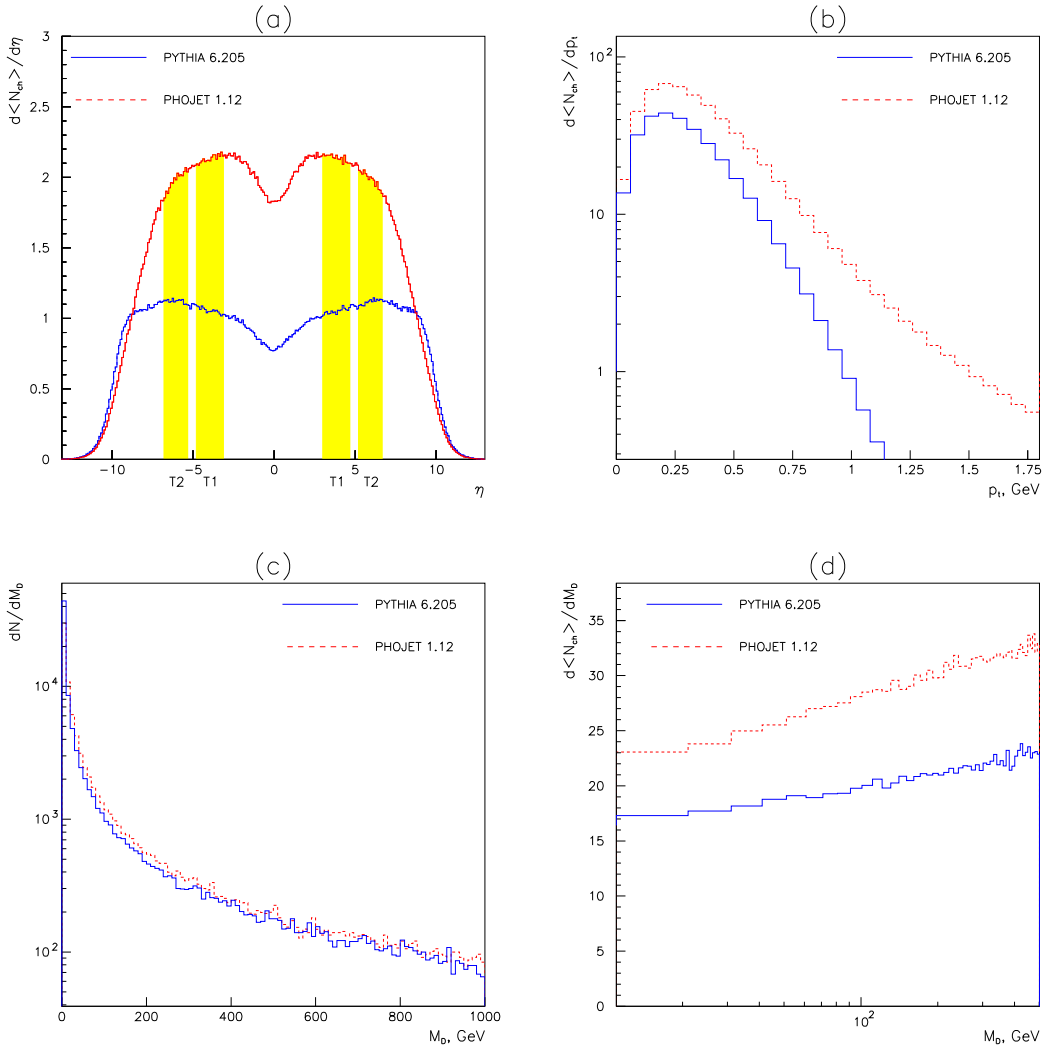

Figure 11: PYTHIA and PHOJET predictions for DD at the LHC energy: (a) charged particles pseudorapidity distribution; (b) charged particles p_t distribution; (c) mass of the diffractive system; (d) average charged particle multiplicity as a function of the diffractive system mass.

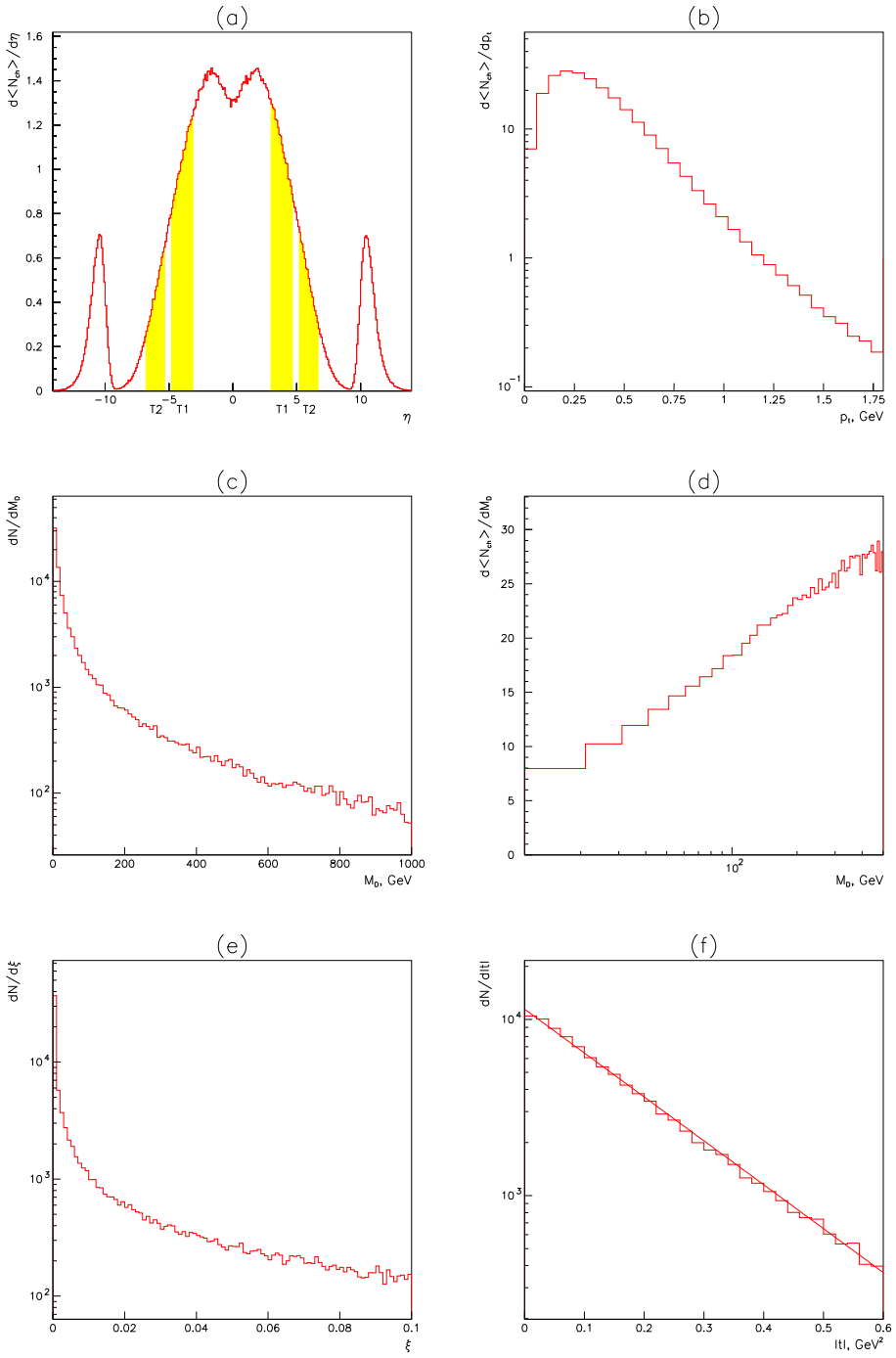

Figure 12: PHOJET predictions for CD at the LHC energy: (a) charged particles pseudorapidity distribution; (b) charged particles p_t distribution; (c) mass of the diffractive system; (d) average charged particle multiplicity as a function of the diffractive system mass; (e) ξ and (f) t distributions of the scattered protons.

Central Diffraction, $\sqrt{s} = 14$ TeV		
	PHOJET	
η areas	$< N_{total} >$/event	$< N_{charged} >$/event
T1F: $3.1 < \eta < 4.7$	2.9	1.7
T2F: $5.3 < \eta < 6.7$	1.3	0.7
All η	27.3	16.7

Table 6: Average particle multiplicity in the diffractive system produced in CD obtained by PHOJET1.12 at the LHC energy for different pseudorapidity areas.

6. Conclusion

We have compared the predictions of the PYTHIA6.205 and PHOJET1.12 MC events generators to available experimental data from the ISR, the SPS and the Tevatron. Also we have compared predictions of PYTHIA6.205 and PHOJET1.12 for minimum bias events and diffractive processes at the LHC energy.

There are large divergencies between PYTHIA and PHOJET in the prediction of the cross sections. They start to differ at energies 600÷700 GeV. The difference in elastic and double diffractive cross sections becomes larger than 50 % at the LHC energy, while the difference in single diffractive and non-diffractive cross sections remains at the level of 22÷23 %. The reason of such a large discrepancy lies in the different models used by PYTHIA and PHOJET for the cross section calculations. Unlike PYTHIA, PHOJET suppresses the diffractive cross sections at high energy providing a reasonable description of the existing experimental data.

On the basis of the comparison of the PYTHIA predictions for the charged particle density in non-single diffractive and inelastic events to the UA5 and CDF data, we would recommend to use the set of parameters called Scenario 3 (see the table 2) for any minimum bias simulation. This scenario of PYTHIA or PHOJET, with its default parameters, give a reasonable description of experimental data at different energies up to 1800 GeV. However, these two generators differ at higher energy and the differencies in predictions become larger with rise of the c.m.energy.

The comparison of PYTHIA and PHOJET simulations to the UA4 data for single diffraction shows that PHOJET describes the diffraction processes better than PYTHIA. Also we have compared PYTHIA and PHOJET for single and double diffraction at the LHC energy. PHOJET predicts ∼2 times larger charged particles multiplicities in the T1 and T2 pseudorapidity areas.

Acknowledgments

The authors are grateful to K.Eggert, M.Bozzo and M.Macrì for helpful discussions. We also thank E. and G. Sobol for their help for the numeralization of some plots with the experimental data.

References

[1] S.N.Ganguli and D.P.Roy Phys.Rep. **67** (1980) 203.

[2] V. Berardi *et al.* CERN-LHCC-2004-002, Jan 2004.

[3] G.Marchesini *et al.*, Comp. Phys. Commun. **67** (1992) 465.

[4] F.E.Paige, S.D.Protopopescu, *ISAJET manual.*

[5] T.Sjöstrand Computer Physics Commun. **82** (1994) 74.

[6] R.Engel *PHOJET manual, V1.05c*, June 1996. Available from: *http* : $//www - ik.fzk.de/$ *engel/phojet.html*.

[7] A.Kupčo, ATL-PHYS-99-019, November 1999.

[8] A.Moraes, I.Dawson and C.Buttar, ATL-PHYS-2003-020, July 2003.

[9] G.Ciapetti and A. di Giaccio, Proceedings of the LHC workshop, vol.2, CERN 90-10, p.155.

[10] G.J.Alner *et al.*, Z. Phys. **C33** (1986) 1.

[11] F.Abe *et al.*, Phys. Rev. **D41(7)** (1990) 2330.

[12] R.K.Ellis and J.C.Sexton, Nucl.Phys. **B269** (1986) 445.

[13] *http://amoraes.home.cern.ch/amoraes/underlying/underlying.html*

[14] A.Capella *et al.*, Phys. Rep. **236** (1994) 227.

[15] A.Donnachie and P.V.Landshoff, Phys.Lett. **B296** (1994) 227.

[16] G.Veneziano, Nucl. Phys. **B74** (1974) 365.

[17] G.F.Chew and C.Rosenzweig, Phys.Rep. **41** (1978) 263.

[18] V.N.Gribov and A.A.Migdal, Sov.J.Nucl.Phys. **8** (1969) 583.

[19] R.Engel, Z.Phys.**C** 66 (1995) 203.

[20] K. Hagiwara *et al.*, Phys. Rev. **D66** (2002). Data files from *http://wwwppds.ihep.su:8001/hadron.html*, courtesy of the COMPAS Group, IHEP, Protvino, Russia.

[21] G.A.Schuler and T.Sjöstrand, Phys.Lett., **B407** (1993) 539.

[22] G.A.Schuler and T.Sjöstrand, Phys.Lett., **B376** (1996) 193.

[23] CNTR Collab., J.Schamberger *et al.*, Phys. Rev. Lett. **34** (1975) 1121.

[24] CHLM Collab., M.G.Albrow *et al.*, Nucl. Phys. **B108** (1976) 1.

[25] CHLM Collab., J.C.M.Armitage *et al.*, Nucl. Phys. **B194** (1982) 365.

[26] CDF Collab., F.Abe *et al.*, Phys. Rev. **D50** (1994) 5535.

[27] UA5 Collab., R.E.Ansorge *et al.*, Z. Phys. **C33** (1986) 175.

[28] E710 Collab., N.A.Amos *et al.*, Phys. Lett. **B301** (1993) 313.

[29] U4 Collab., D.Bernard *et al.*, Phys. Lett. **B166** (1986) 459.